ACS OMEGA

http://pubs.acs.org/journal/acsodf

Article

Effects of Oxygen: Experimental and VTST/DFT Studies on Cumene Autoxidation with Air under Atmospheric Pressure

Yufeng Wu,* Jingnan Zhao, Qingwei Meng,* Mingshu Bi, Cunfei Ma, and Zongyi Yu

Cite This: *ACS Omega* 2022, 7, 34547−34553

Read Online

ACCESS | Metrics & More | Article Recommendations | Supporting Information

ABSTRACT: The mechanism of how oxygen affects cumene autoxidation related to temperature is still bewildering. Kinetic analysis of cumene autoxidation with air at a pressure of 1.0 atm was investigated by experiments and variational transition state theory/DFT. Oxygen was the limiting factor for cumene autoxidation above 100 °C, although it had negligible impacts on cumene autoxidation at 70−100 °C. The kinetic analysis by VTST coupled with DFT calculations proved that $\{k_{6,\text{reverse}}[\text{ROO}^\bullet]\}/\{k_{7,\text{forward}}[\text{RH}]_0\,[\text{ROO}^\bullet]\} > 10^3$ (70−120 °C), suggesting that ROO• tended to decompose back to R• and O_2 rapidly, whereas it was much slower for ROO• abstracting a hydrogen atom from RH to form ROOH. When the concentration of oxygen was higher than the critical value ($[O_2]_{\text{critical}}$), it could not significantly affect the equilibrium concentration of ROO•, which in turn could not affect the autoxidation rate significantly. Besides, the critical oxygen concentration ($[O_2]_{\text{critical}}$) was exponentially related to $1/T$, which was consistent with Hattori's experimental results.

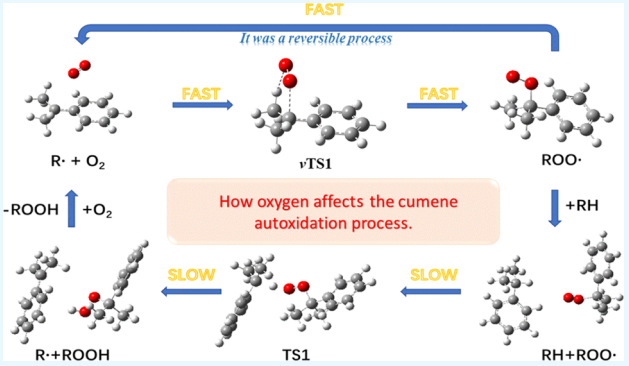

1. INTRODUCTION

Oxidations with molecular oxygen are awfully fascinating that often address the priorities of green and sustainable chemistry.[1,2] At present, molecular oxygen has been successfully used in oxidations of alkenes, alcohols, thioethers, and amines.[1,3] One prominent industrial example is cumene autoxidation to prepare cumene hydroperoxide (ROOH), which was then converted into phenol with a production of more than 11.4×10^6 t/a in 2013.[4] The peroxidation processes had also swept the industry[5] because coproduct processes (PO/SM and PO/TBA) and the Sumitomo process[6] had been widely used in the industrial production of propylene oxide, which was the synthetic material for polyurethane foams and polyester resins.[7]

Cumene autoxidation is a typical heterogeneous gas−liquid reaction and attracts considerable attention.[8−12] The mechanisms and kinetic study of cumene autoxidation have received extensive attention.[2,8,13−15] An intricate series of elementary reactions, in Scheme 1, were involved in cumene autoxidation. Generally, it was deemed that reaction 7, which was not related to oxygen, was slower and thus the decisive step to the chain reaction.[4] Nevertheless, oxygen was undoubtedly one of the major factors and has attracted a lot of attention.[16,17] Hattori et al.[16] found that the oxidation rate constant was not affected by oxygen when the partial pressure of oxygen in the gas phase was higher than a certain value. Ulitin et al.[17] found that the oxygen mass transfer rate did not affect the accumulation rate of ROOH under reaction conditions of 1.013×10^5 Pa and 110 °C. Instead, when the concentration of oxygen dissolved in

Scheme 1. Kinetic Scheme of Cumene Autoxidation

◆ Chain initiation

(1) $RH+O_2 \xrightarrow{k_1} R\bullet+HOO\bullet$ (2) $ROOH \xrightarrow{k_2} RO\bullet+HO\bullet$

(3) $2ROOH \xrightarrow{k_3} ROO\bullet+RO\bullet+H_2O$

◆ Chain propagation

(4) $RH+RO\bullet \xrightarrow{k_4} ROH+R\bullet$ (5) $RH+HO\bullet \xrightarrow{k_5} H_2O+R\bullet$

(6) $R\bullet+O_2 \xrightarrow{k_6} ROO\bullet$ (7) $RH+ROO\bullet \xrightarrow{k_7} ROOH+R\bullet$

(8) $ROOH+RO\bullet \xrightarrow{k_8} ROH+ROO\bullet$ (9) $RO\bullet \xrightarrow{k_9} C_6H_5C(O)CH_3+CH_3\bullet$

(10) $CH_3\bullet+O_2 \xrightarrow{k_{10}} CH_3OO\bullet$ (11) $CH_3OO\bullet+RH \xrightarrow{k_{11}} CH_3OOH+R\bullet$

(12) $2ROO\bullet \xrightarrow{k_{12}} 2RO\bullet+O_2$ (13) $HOO\bullet+RH \xrightarrow{k_{13}} HOOH+R\bullet$

◆ Chain termination

(14) $2R\bullet \xrightarrow{k_{14}} RR$ (15) $R\bullet+ROO\bullet \xrightarrow{k_{15}} ROOR$

(16) $2ROO\bullet \xrightarrow{k_{16}} ROOR+O_2$ (17) $R\bullet+HOO\bullet \xrightarrow{k_{17}} ROOH$

(18) $CH_3OO\bullet+ROO\bullet \xrightarrow{k_{18}} ROH+HC(O)H+O_2$

Received: July 10, 2022
Accepted: September 6, 2022
Published: September 19, 2022

cumene was higher than a value that was linear with the concentration of the initiator (ROOH), there was a weak dependence of ROOH's accumulation rate on oxygen. Thus, the boundary concentration of oxygen related to temperature, to distinguish whether the oxygen affects cumene autoxidation, is of great valuable, but no relevant reports have been found.

Here, kinetic analysis of cumene autoxidation with air as oxidant was carried out through experiments and variational transition state theory (VTST) coupled with density functional theory (DFT) calculations. Both the forward and reverse reactions were analyzed by VTST coupled with DFT calculations, providing good insights into how oxygen affects cumene autoxidation. Besides, the critical oxygen concentration $[O_2]_{critical}$ related to temperature was present in this work, providing theoretical and technical supports for cumene autoxidation.

2. EXPERIMENTAL AND CALCULATIONS

2.1. Materials. Unless otherwise stated, all commercial reagents and solvents were used without further purification. Cumene (>99% purity, 0.47 mol % of ROOH was determined by ^{1}H NMR) was produced by Institute of Guangfu Fine Chemicals. K_2CO_3 was produced by Xilong Chemical Co., Ltd. ^{1}H NMR (400 MHz) spectra were recorded on a Bruker Avance II 400 spectrometer.

2.2. Cumene Autoxidation. Figure 1 illustrates the setup utilized in the experimental work. The reactor was a 50 mL

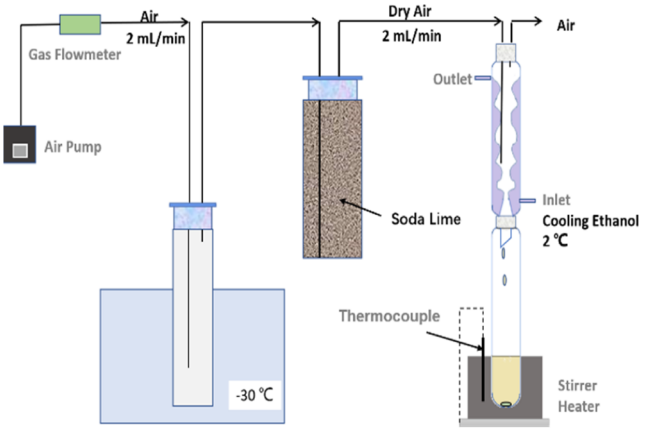

Figure 1. Cumene autoxidation experimental scheme.

reaction tube (outer diameter of 23 mm). K_2CO_3 (0.5 mmol, 69.1 mg), cumene (3 mL), and a magnetic stirring bar (1 cm) were successively added to the reaction tube, which was then put onto a metal plate above a magnetic stirring apparatus (IKA Plate, RCT digital). Then, the reflux unit and dry air preparation unit were connected as shown in Figure 1. K_2CO_3 was used to neutralize the organic acid generated in situ, preventing the decomposition of ROOH promoted by organic acid.[18] The effects of K_2CO_3 on cumene autoxidation are further discussed in the Supporting Information. To ensure that the ratio of O_2 and N_2 over the surface of reaction liquor is stable, drying air (2 mL/min) was fed into the gas phase continuously. The reaction proceeded at a specific temperature (70, 80, 90, 100, 110, and 120 °C). The samples were sampled on time and diluted immediately with DMSO-d_6. Conversion and selectivity were determined by ^{1}H NMR. Dry air was prepared by the following steps: the air flowed into the reaction system through a pump and a gas flowmeter (set as 2.0 mL/min) and was successively dried with condensation at −30 °C and soda lime.

2.3. Kinetic Model of Cumene Autoxidation. Based on the mechanisms of alkanes' autoxidation,[17] a kinetic scheme of cumene autoxidation proceeds by a chain mechanism including chain initiation, chain propagation, and chain termination (Scheme 1). According to Figure S4, high selectivities (>90%) were obtained at conversions less than 8%. Thus, side reactions were ignored here. The generation rate of ROOH was mainly determined by reaction 7 and thus eq 1 was used to describe the generation rate of ROOH.

$$r_{ROOH} = -r_{RH} = k_7[ROO^\bullet][RH] \quad (1)$$

where $[ROO^\bullet]$ and $[RH]$ are the concentration of $ROO^\bullet$ and cumene, mol/L, respectively and k_7 is the reaction constant for reaction 7.

2.4. Computational Details. All geometry optimizations of the reactants, transition states, intermediates, and products were carried out with the Gaussian 16 program. The B3LYP[19,20] hybrid exchange−correlation functional with 6-311 + g(d,p) basis set was applied for geometrical optimizations and subsequent frequency calculations. The optimizations were carried out at 378.15 K using cumene as the solvent. No imaginary frequencies were found in the vibrational spectra of all reactants, intermediates, and products. Only one imaginary frequency corresponding to the reaction coordinates was found for the transition states. The intrinsic reaction coordinate calculations were carried out to further verify the relationship between the reactants, transition states, and products. The rate constant for the barrierless $R^\bullet + O_2$ reaction were treated as Silva's literature,[21] using VTST coupled with DFT calculations. The two-parameters Arrhenius formula to calculate the rate constants related to temperature for elementary reactions were obtained from KISTHELP software.[22]

3. RESULTS AND DISCUSSION

3.1. Saturated Solubility of Oxygen. According to Hattori's report,[16] the concentration of oxygen dissolved in cumene did not affect the reaction rate of cumene autoxidation at a temperature below 120 °C when the concentration of dissolved oxygen was greater than 7×10^{-4} mol/L. This concentration corresponds to an equilibrium partial pressure of 0.1 bar in the gas phase.[4] To verify whether oxygen affected cumene autoxidation, the oxygen solubility in cumene was calculated based on the gas−liquid equilibrium theory and Hayduk's semiempirical method[23−25] at first. The detailed calculation process is present in the Supporting Information. When the reaction was performed with air as the oxidant under a pressure of 1.013×10^5 Pa, the oxygen partial pressure, p_{oxygen}, was calculated and the results are listed in Table S1, suggesting that the oxygen partial pressure decreased with the increasing temperature. The mole fraction of oxygen (X_T) in cumene under an oxygen partial pressure of 1.0 bar at different temperatures was about 10.9×10^{-4} and had a negligible temperature coefficient (Table S1). This result was consistent with Low's literature.[26] When air was used as the oxidant, the molar concentration of oxygen ($[O_2]_T^S$) at 70−120 °C was calculated and is depicted in Figure 2. There was a clear downward trend (decreased from 12.84×10^{-4} to 7.40×10^{-4} mol/L) for $[O_2]_T^S$ when the temperature increased from 70 to

https://doi.org/10.1021/acsomega.2c04362
ACS Omega 2022, 7, 34547−34553

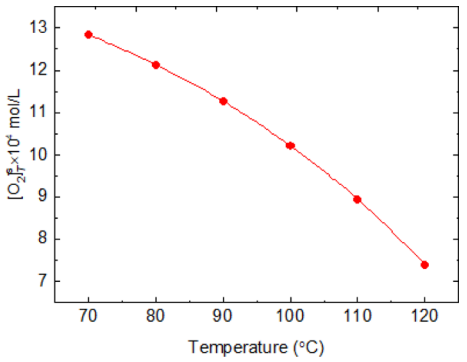

Figure 2. Molar concentration of oxygen ($[O_2]_T^S$) dissolved in cumene in an air atmosphere.

120 °C. Therefore, the influence of oxygen on cumene autoxidation under experimental conditions could be neglected because $[O_2]_T^S$ was greater than 7×10^{-4} mol/L at 70−120 °C.

3.2. Kinetic Study of Cumene Autoxidation without Considering the Oxygen Solubility. Based on the above analysis, the influence of oxygen on cumene autoxidation under experimental conditions could be neglected. Therefore, reaction 7 was the rate-controlling step for cumene autoxidation. According to the assumption of pseudo-steady-state,[13] $k_7[ROO^\bullet][RH] = k_6[R^\bullet][O_2]$ could be obtained when ignoring the side reactions. $g(T)$ was assumed as the total concentration of radicals and $[ROO^\bullet] + [R^\bullet] \approx g(T)$. Then, eq 2 was derived to calculate the concentration of ROO•. The values of $[ROO^\bullet]/g(T)$ at different temperatures were first calculated using parameters from Somma's report[15] ($\log k_{70} = 7.6$, $\log k_{60} = 8.4$, $\Delta E_{a6} = 0$, and $\Delta E_{a7} = 53.16$ kJ/mol) and the results are listed in Table S2. The value of $[ROO^\bullet]/g(T)$ decreased from 0.9997 to 0.9946 when the temperature increased from 70 to 120 °C, suggesting that the concentration of ROO• was close to the total concentration of radicals independent of temperature. Thus, the effect of temperature on the reaction rate will be much more pronounced than $[ROO^\bullet]$ at 70−120 °C.

$$[ROO^\bullet] = \frac{g(T)}{1 + \frac{k_{70}}{k_{60}}\frac{[RH]}{[O_2]}\exp\left(\frac{\Delta E_{a6} - \Delta E_{a7}}{RT}\right)} \quad (2)$$

To simplify the kinetic study of cumene autoxidation, a hypothesis that the concentration of ROO• was not sensitive to temperature at 70−120 °C and K_1 (= $k_7[ROO^\bullet]$) was introduced. Eq 1 was rewritten as eq 3 to study the reaction kinetics between ROO• and RH, indicating that $\ln(1-x)$ and t have a linear relationship. x is the conversion of cumene. The regression lines and equations of $\ln(1-x)$ with t at 70−120 °C are shown in Figure S3 and listed in Table S3. The values of K_1 at different temperatures were equal to the corresponding slopes of the regression lines as shown in Figure S3. $\ln K_1$ and $1/T$ should have a linear relationship according to Arrhenius eq 4. Unexpectedly, as shown in Figure 3a, $R^2 = 0.89927$ was obtained for the linear regression of $\ln K_1$ and $1/T$ in the temperature range of 70−120 °C, suggesting a poor reliability. Figure 3b also showed that $\ln K_1$ and $1/T$ were linear with a good degree of reliability in the temperature ranges of 70−100 and 100−120 °C with $R^2 = 0.98218$ and $R^2 = 0.92307$, respectively. The slope value in the temperature range of 70−100 °C was obviously greater than that in the temperature range of 100−120 °C. Same situation was discovered in

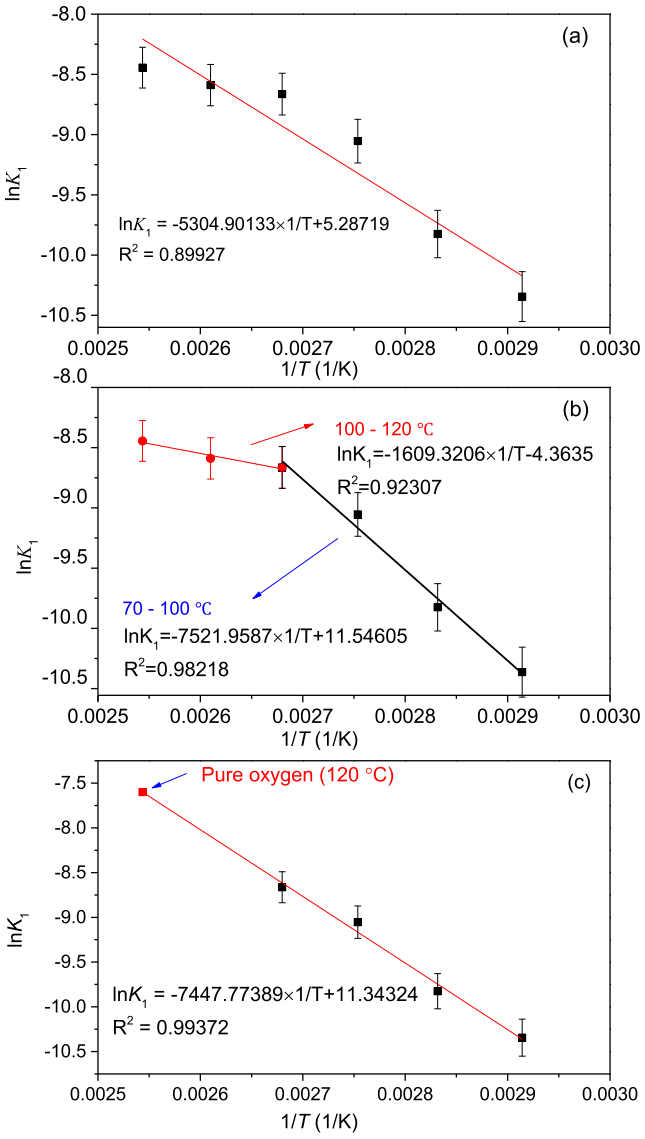

Figure 3. Linear regression analysis of ln K_1 with $1/T$, with error bars of 2%. (a) temperature range of 70−120 °C; (b) temperature range of 70−100 and 100−120 °C, respectively; and (c) pure oxygen and air were used as the oxidant at 120 and 70−100 °C, respectively.

Koshel's report[8] and they deemed that the activity of PINO• may be different in the two temperature ranges. From this perspective, the activation energy of reaction 7 were 62.54 and 13.38 kJ/mol in the temperature ranges of 70−100 and 100−120 °C, respectively. However, in our opinion, the change of oxygen concentration in the reaction liquor may lead to this situation as well. Figure S4c,d also indicated that the cumene autoxidation rate at 120 °C significantly increased using high purity oxygen instead of air, indicating oxygen was the limiting factor at 120 °C. Notably, $R^2 = 0.99372$ as shown in Figure 3c was obtained for the linear regression analysis of $\ln K_1$ with $1/T$ when the value of K_1 at 120 °C using high purity oxygen as the oxidant was used. Therefore, the concentration of oxygen was the limiting factor for cumene autoxidation above 100 °C, although it had negligible effects on cumene autoxidation at 70−100 °C. Based on Figure 3c, the activation energy of reaction 7 was 61.92 kJ/mol.

$$\ln(1 - x) = -K_1 t \quad (3)$$

https://doi.org/10.1021/acsomega.2c04362
ACS Omega 2022, 7, 34547−34553

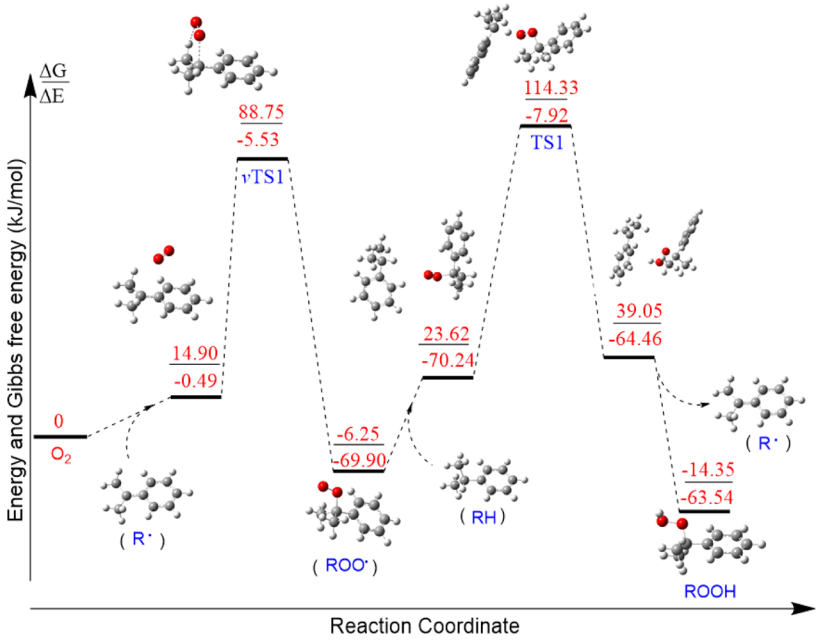

Figure 4. Energy and Gibbs free energy profile (at 378.15 K) for cumene autoxidation, calculated at B3LYP/6-311 + G(d,p) level of theory.

$$\ln K_1 = \ln K_{10} - \frac{\Delta E_{a7}}{RT} \quad (4)$$

3.3. Kinetic Study by VTST/DFT Calculations. Kozuch and Martin[27] have reported that there are no rate-determining steps, only rate-determining states. Inspired by Kozuch's report, we believe that there may be new breakthroughs in the in-depth study of kinetics from the perspective of transition state theory and reversible reactions. Here, the energy and Gibbs free energy profile (at 378.15 K) for cumene autoxidation, calculated at B3LYP/6-311 + G(d,p) level of theory, is depicted in Figure 4. Potential energy surface scan results (Figure S5) showed that the reaction of O_2 with R$^\bullet$ to form ROO$^\bullet$ is barrierless. It was consistent with the previous reports[28−30] that the reaction of alkyl radicals with oxygen was barrierless. Rate constants for R$^\bullet$ + O_2 at each point along the potential energy surface were calculated and are depicted in Figure S6. The location of the variational transition state (***ν*TS1**) is at a R−OO bond length of 2.43 Å. As a result, activation free energy barriers of 88.75 and 95.00 kJ/mol were required for the reaction of O_2 with R$^\bullet$ to form ROO$^\bullet$ and its reversible reaction, respectively. Only one imaginary frequency (91.82*i*) was found for ***ν*TS1**. The process that ROO$^\bullet$ abstracted a hydrogen atom from RH required to overcome an activation free energy barrier of 120.58 kJ/mol and only one imaginary frequency (1766.35*i*) was found for **TS1**. The Gibbs free energy change for the entire reaction was −14.35 kJ/mol, suggesting a feasible process.

Two-parameters Arrhenius formulas were used to calculate the minimum rate constants related to temperature for the main elementary reactions and its reversible reactions, using VTST coupled with the B3LYP/6-311 + G(d,p) level of theory in the temperature range of 343.15−398.15 K. The corresponding parameters are listed in Table 1. The fitted activation energy (61.58 kJ/mol) for reaction 7 was close to our experimental value (61.92 kJ/mol). Interestingly, it was also found that $\{k_{6,\text{reverse}}[\text{ROO}^\bullet]\}/\{(k_{7,\text{forward}}[\text{RH}]_0)\ [\text{ROO}^\bullet]\} > 10^3$ (70−120 °C), suggesting that the rate for the reverse reaction of reaction 6 was much faster than that for the forward reaction of reaction 7. Thus, the reverse reaction of reaction 6 should not be ignored in the kinetic study of cumene autoxidation. Denisov and Afanas'ev[31] have also reported that some peroxyl radicals, such as cyclohexadienyl peroxyl radicals, have a weak C−OO bond and decompose back to R$^\bullet$ and O_2. It was consistent with our results. Nevertheless, the addition reaction of O_2 to R$^\bullet$ was regarded as a one-way reaction process in the previous kinetic studies of cumene autoxidation.[8,13,16]

Table 1. Kinetic Parameters for the Reactions 6 and 7 at 343.15−398.15 K

elementary reactions	*A*	*E* (kJ/mol)
$R^\bullet + O_2 \xrightarrow{k_{6,\text{forward}}} ROO^\bullet$	9.62×10^6	−8.91
$ROO^\bullet \xrightarrow{k_{6,\text{reverse}}} R^\bullet + O_2$	3.87×10^{14}	69.44
$ROO^\bullet + RH \xrightarrow{k_{7,\text{forward}}} ROOH + R^\bullet$	7.50×10^8	61.58
$ROOH + R^\bullet \xrightarrow{k_{7,\text{reverse}}} ROO^\bullet + RH$	1.38×10^9	47.53

The reaction rates for those elementary reactions consuming ROO$^\bullet$, such as reactions 12, 15, and 16, were of course much slower than reaction 7. Therefore, eq 5 was used to describe that the generation rate of ROO$^\bullet$ was equal to its consumption rate in view of the quasi-steady-state assumption. Because $k_{6,\text{reverse}}/(k_{7,\text{forward}}[\text{RH}]_0) > 10^3$ and $k_{6,\text{forward}}[O_2]/k_{7,\text{reverse}} > 10^6$, eq 6 was used to calculate the ratio of R$^\bullet$ and ROO$^\bullet$. It was clear that the ratio of R$^\bullet$ and ROO$^\bullet$ was mainly determined by temperature and the oxygen concentration. Both increasing the concentration of O_2 and decreasing temperature could lead to a decrease of the ratio of R$^\bullet$ and ROO$^\bullet$. When the concentration of oxygen was higher than the critical value ($[O_2]_{\text{critical}}$), it could not significantly affect the equilibrium concentration of ROO$^\bullet$, which in turn could not affect the autoxidation rate significantly. Eq 7 was derived to calculate K_1 ($= k_{7,\text{forward}}[\text{ROO}^\bullet]$). Interestingly, as shown in Figure 5, the

https://doi.org/10.1021/acsomega.2c04362
ACS Omega 2022, 7, 34547−34553

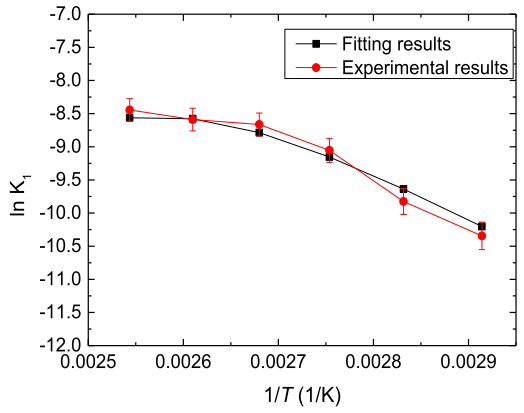

Figure 5. Plot of $\ln K_1$ over $1/T$, set error bars of 2% for the experimental results.

curve of $\ln K_1$ over $1/T$ for the fitting results (when $g(T) = 1.21 \times 10^{-4}$ mol/L) was consistent with our experimental results.

$$k_{6,\text{forward}}[R^{\bullet}][O_2] + k_{7,\text{reverse}}[R^{\bullet}][\text{ROOH}] = k_{7,\text{forward}}[\text{ROO}^{\bullet}][\text{RH}] + k_{6,\text{reverse}}[\text{ROO}^{\bullet}] \quad (5)$$

$$\frac{[R^{\bullet}]}{[\text{ROO}^{\bullet}]} \approx \frac{k_{6,\text{reverse}}}{k_{6,\text{forward}}[O_2]} = \frac{4.0 \times 10^7 \exp(-9423.4/T)}{[O_2]} \quad (6)$$

$$K_1 = k_{7,\text{forward}}[\text{ROO}^{\bullet}] = \frac{k_{7,\text{forward}}g(T)}{1 + [R^{\bullet}]/[\text{ROO}^{\bullet}]} \quad (7)$$

3.4. Mathematical Model to Calculate the Critical Concentration of Oxygen. Both Hattori[16] and Ulitin[17] found that there was a weak dependence of ROOH's accumulation rate on oxygen when the oxygen concentration or the partial pressure of oxygen was higher than some value. To our knowledge, there were no reports to solve the general critical oxygen concentration related to temperature. According to eqs 6 and 7, the value of $\{k_{7,\text{forward}}[\text{ROO}^{\bullet}]\}$, as well as the ROOH's accumulation rate, will increase with increase of $[O_2]$. The closer the ratio of $R^{\bullet}$ and $\text{ROO}^{\bullet}$ is to 0, the closer the reaction rate is to the maximum reaction rate. When the concentration of oxygen was higher than the critical value ($[O_2]_{\text{critical}}$), it could not significantly affect the concentration of $\text{ROO}^{\bullet}$ by increasing oxygen concentration, which in turn could not affect the autoxidation rate significantly. We assumed that when $[R^{\bullet}]/[\text{ROO}^{\bullet}] \le m$, there is a weak dependence of ROOH's accumulation rate on oxygen. This is to say "m" can be regarded as a threshold ($\{[R^{\bullet}]/[\text{ROO}^{\bullet}]\}_{\text{threshold}} = m$) to judge whether the concentration of oxygen could affect the autoxidation rate. Eq 8, to solve the critical oxygen concentration ($[O_2]_{\text{critical}}$), could be derived from eq 6. m is recommended to be in the range of 0.1−0.20. Similarly, the critical oxygen partial pressure was also exponentially related to $1/T$, when the saturated vapor pressure of cumene was ignored.

$$[O_2]_{\text{critical}} = \frac{4.0 \times 10^7}{m}\exp(-9423.4/T) \quad (8)$$

Hattori[16] reported that the rate constant K and the partial pressure of oxygen obey the function of $K = MP_{O_2}/(1 + NP_{O_2})$. Thus, the maximum value of K ($K_{\max}$) would be infinitely close to M/N. We assumed that there was a weak dependence of cumene autoxidation on oxygen when K was 0.85 times $K_{\max}$ (i.e., $m = 0.1765$). Thus, the critical oxygen partial pressures related to temperature were calculated ($P_{O_2,\text{critical}}$: 110 °C, 0.157 atm; 120 °C, 0.241 atm; and 130 °C, 0.327 atm). Interestingly, $\ln P_{O_2,\text{critical}}$ and $1/T$ were linear with a good degree of reliability ($R^2 = 0.9968$) in the temperature range of 110−130 °C (Figure 6). Therefore, $P_{O_2,\text{critical}} = 4.25 \times 10^5 \exp(-5668.73/T)$ or $[O_2]_{\text{critical}} \approx 2.96 \times 10^4 \exp(-5668.73/T)$. This result was consistent with our derivation that the critical oxygen partial pressure was exponentially related to $1/T$ though some differences existed between the experimental results and theoretical derivations. We deemed that the difference was mainly caused by the conditions of the experiments using a bubble column reactor, where the oxygen partial pressure gradually decreases from bottom to top of the reaction system. Besides, the saturated vapor pressure of cumene was not considered in Hattori's report, which may result in this difference as well.

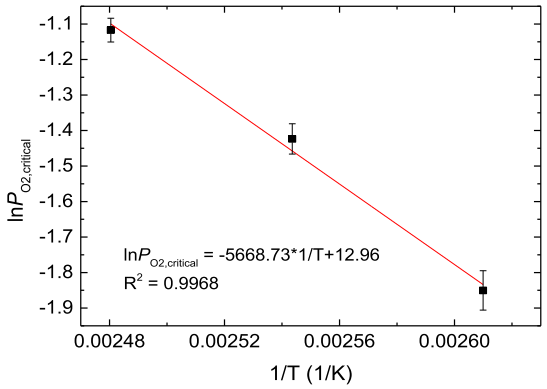

Figure 6. Linear regression analysis of $\ln P_{O_2,\text{critical}}$ and $1/T$ in the temperature range of 110−130 °C, set error bars of 3%.

4. CONCLUSIONS

In conclusion, kinetic analysis of cumene autoxidation with dry air as the oxidant under conditions of 70−120 °C and 1.0 atm was studied by experiments and VTST/DFT calculations. Oxygen was the limiting factor for the rate constant of cumene autoxidation above 100 °C, although it had negligible impact on cumene autoxidation at 70−100 °C. The reaction rate at 120 °C was significantly increased by using high purity oxygen instead of air. Reaction 6 was reversible in the view of VTST coupled with DFT calculations, thus determining the equilibrium concentration of $\text{ROO}^{\bullet}$. It provides good insights into how oxygen affects cumene autoxidation. Finally, the critical oxygen concentration ($[O_2]_{\text{critical}}$) grew exponentially with $1/T$. It was consistent with Hattori's experimental results.

■ ASSOCIATED CONTENT

Supporting Information

The Supporting Information is available free of charge at https://pubs.acs.org/doi/10.1021/acsomega.2c04362.

Saturated solubility of oxygen calculated by Hayduk's semiempirical method and gas−liquid equilibrium theory; effects of K_2CO_3 on cumene autoxidation;

https://doi.org/10.1021/acsomega.2c04362
ACS Omega 2022, 7, 34547−34553

calculation results for $[ROO^{\bullet}]/g(T)$ at 70−120 °C; conversion of cumene (x) over t; linear regression of $\ln(1-x)$ with t; curves of conversion and selectivity with time at 80, 100, and 120 °C; reaction rate for $R^{\bullet} + O_2$ calculated by VTST coupled with DFT calculations; and DFT calculations for the main processes for cumene autoxidation (PDF)

AUTHOR INFORMATION

Corresponding Authors

Yufeng Wu − *School of Chemical Engineering, Dalian University of Technology, Dalian, Liaoning 116024, China*; orcid.org/0000-0002-2404-0053; Email: wuyufeng@dlut.edu.cn

Qingwei Meng − *School of Chemical Engineering, Dalian University of Technology, Dalian, Liaoning 116024, China*; orcid.org/0000-0002-1743-2518; Email: mengqw@dlut.edu.cn

Authors

Jingnan Zhao − *School of Chemical Engineering, Dalian University of Technology, Dalian, Liaoning 116024, China*

Mingshu Bi − *School of Chemical Engineering, Dalian University of Technology, Dalian, Liaoning 116024, China*

Cunfei Ma − *School of Chemical Engineering, Dalian University of Technology, Dalian, Liaoning 116024, China*

Zongyi Yu − *School of Chemical Engineering, Dalian University of Technology, Dalian, Liaoning 116024, China*

Complete contact information is available at: https://pubs.acs.org/10.1021/acsomega.2c04362

Notes

The authors declare no competing financial interest.

ACKNOWLEDGMENTS

This work was supported by the National Regional Innovation Joint Fund (U20A20143), Organization Department of Liaoning Province (XLYC1902086), Dalian Science and Technology Bureau (2019J1CY006), and Dalian University of Technology Fundamental Research Fund (DUT21RC(3) 016). The authors also thank the State Key Laboratory of Fine Chemicals and the Network and Information Center of the Dalian University of Technology for their support.

REFERENCES

(1) Jiao, N.; Stahl, S. S. *Green Oxidation in Organic Synthesis*; John Wiley & Sons, 2019.

(2) Suresh, A. K.; Sharma, M. M.; Sridhar, T. Engineering aspects of industrial liquid-phase air oxidation of hydrocarbons. *Ind. Eng. Chem. Res.* **2000**, *39*, 3958−3997.

(3) Teles, J. H.; Hermans, I.; Franz, G.; Sheldon, R. A. Oxidation. *Ullmann's Encyclopedia of Industrial Chemistry*; Wiley Online Library, 2015; pp 1−103.

(4) Weber, M.; Daldrup, J.-B. G.; Weber, M. Noncatalyzed Radical Chain Oxidation: Cumene Hydroperoxide. *Liquid Phase Aerobic Oxidation Catalysis: Industrial Applications and Academic Perspectives*; John Wiley & Sons, 2016; pp 15−31.

(5) Mccoy, M. New routes to propylene oxide. *Chem. Eng. News* **2001**, *79*, 19−20.

(6) Tsuji, J.; Yamamoto, J.; Ishino, M.; Oku, N. Development of new propylene oxide process. *Sumitomo Kagaku* **2006**, *1*, 4−10.

(7) Khatib, S. J.; Oyama, S. T. Direct oxidation of propylene to propylene oxide with molecular oxygen: A review. *Catal. Rev.* **2015**, *57*, 306−344.

(8) Sapunov, V. N.; Kurganova, E. A.; Koshel, G. N. Kinetics and mechanism of cumene oxidation initiated by N-Hydroxyphthalimide. *Int. J. Chem. Kinet.* **2018**, *50*, 3−14.

(9) Petroselli, M.; Melone, L.; Cametti, M.; Punta, C. Lipophilic N-Hydroxyphthalimide Catalysts for the Aerobic Oxidation of Cumene: Towards Solvent-Free Conditions and Back. *Chem.—Eur. J.* **2017**, *23*, 10616−10625.

(10) Amorati, R.; Lucarini, M.; Mugnaini, V.; Pedulli, G. F.; Minisci, F.; Recupero, F.; Fontana, F.; Astolfi, P.; Greci, L. Hydroxylamines as oxidation catalysts: Thermochemical and kinetic studies. *J. Org. Chem.* **2003**, *68*, 1747−1754.

(11) Yang, W. J.; Guo, C. C.; Tao, N. Y.; Cao, J. Aerobic oxidation of cumene to cumene hydroperoxide catalyzed by metalloporphyrins. *Kinet. Catal.* **2010**, *51*, 194−199.

(12) Xu, S. A.; Huang, C. P.; Zhang, J.; Chen, B. H. Catalytic activity of Cu/MgO in liquid phase oxidation of cumene. *Korean J. Chem. Eng.* **2009**, *26*, 1568−1573.

(13) Bhattacharya, A. Kinetic modeling of liquid phase autoxidation of cumene. *Chem. Eng. J.* **2008**, *137*, 308−319.

(14) Di Somma, I.; Marotta, R.; Andreozzi, R.; Caprio, V. Detailed thermal and kinetic modeling of cumene hydroperoxide decomposition in cumene. *Process Saf. Environ. Prot.* **2013**, *91*, 262−268.

(15) Di Somma, I.; Marotta, R.; Andreozzi, R.; Caprio, V. Dicumyl peroxide thermal decomposition in cumene: Development of a kinetic model. *Ind. Eng. Chem. Res.* **2012**, *51*, 7493−7499.

(16) Hattori, K.; Tanaka, Y.; Suzuki, H.; Ikawa, T.; Kubota, H. Kinetics of liquid phase oxidation of cumene in bubble column. *J. Chem. Eng. Jpn.* **1970**, *3*, 72−78.

(17) Kharlampidi, K. E.; Tereshchenko, K. A.; Nurmurodov, T. S.; Shiyan, D. A.; Miroshkin, N. P.; Ziyatdinov, N. N.; Ziganshina, A. S.; Nurullina, N. M.; Khursan, S. L.; Ulitin, N. V. The kinetic modeling of cumene oxidation taking into account oxygen mass transfer. *Chem. Eng. J.* **2020**, *392*, 123811.

(18) Jun, L. Research progress in the catalysts for cumene catalytic oxidation. *Ind. Catal.* **2014**, *22*, 173−180.

(19) Becke, A. Density-Functional Thermochemistry. III. The Role of Exact Exchange. *J. Chem. Phys.* **1993**, *98*, 5648−5652.

(20) Lee, C.; Yang, W.; Parr, R. G. Development of the Colle-Salvetti correlation-energy formula into a functional of the electron density. *Phys. Rev. B: Condens. Matter Mater. Phys.* **1988**, *37*, 785.

(21) da Silva, G.; Bozzelli, J. W. Kinetic modeling of the benzyl + HO2 reaction. *Proc. Combust. Inst.* **2009**, *32*, 287−294.

(22) Canneaux, S.; Bohr, F.; Henon, E. KiSThelP: A Program to Predict Thermodynamic Properties and Rate Constants from Quantum Chemistry Results†. *J. Comput. Chem.* **2014**, *35*, 82−93.

(23) Hayduk, W.; Buckley, W. D. Temperature coefficient of gas solubility for regular solutions. *Can. J. Chem. Eng.* **1971**, *49*, 667−671.

(24) Hayduk, W.; Castaneda, R. Solubilities of the highly soluble gases, propane and butane, in normal paraffin and polar solvents. *Can. J. Chem. Eng.* **1973**, *51*, 353−358.

(25) Barton, A. Gases. In *CRC Hand Book of Solubility Parameters and Other Cohesion Parameters*, 2nd ed.; Barton, A. F. M., Ed.; CRC Press LLC: United States of America, 1991; Chapter 11, pp 321−340.

(26) Low, D. I. R. The unsteady state absorption of oxygen in cumene. *Can. J. Chem. Eng.* **1967**, *45*, 166−170.

(27) Kozuch, S.; Martin, J. M. L. The Rate-Determining Step is Dead. Long Live the Rate-Determining State. *ChemPhysChem* **2011**, *12*, 1413−1418.

(28) Goldsmith, C. F.; Green, W. H.; Klippenstein, S. J. Role of O-2 + QOOH in Low-Temperature Ignition of Propane. 1. Temperature and Pressure Dependent Rate Coefficients. *J. Phys. Chem. A* **2012**, *116*, 3325−3346.

(29) Miller, J. A.; Klippenstein, S. J. The reaction between ethyl and molecular oxygen II: Further analysis. *Int. J. Chem. Kinet.* **2001**, *33*, 654−668.

(30) Clifford, E. P.; Farrell, J. T.; DeSain, J. D.; Taatjes, C. A. Infrared frequency-modulation probing of product formation in alkyl plus O-2 reactions: I. The reaction of C2H5 with O-2 between 295 and 698 K. *J. Phys. Chem. A* **2000**, *104*, 11549−11560.

(31) Afanas'ev, I. B.; Denisov, E. T. Chain Mechanism of Liquid-Phase Oxidation of Hydrocarbons. *Oxidation Antioxidants in Organic Chemistry Biology*; CRC Press: Boca Raton, London, New York, Singapore, 2005; pp 61−122.

https://doi.org/10.1021/acsomega.2c04362
ACS Omega 2022, 7, 34547−34553